Supporting Information

Switchable photoluminescence of europium(III) complexes with chromonylhydrazones

Asahi Kamei,[a] Daisuke Saito,[b,c] Kazuma Takahara,[d] Keito Nose,[a] Hideki Okamoto,[e] Masaki Yoshida,[f] Masako Kato,[c,g] Takayoshi Suzuki[a,h,]*

[a] Graduate School of Environmental, Life, Natural Science and Technology, Okayama University, Okayama 700-8530, Japan.

[b] Graduate School of Science, Hokkaido University, Kita 10 Nishi 8, Kita-ku, Sapporo 060-0810, Japan.

[c] School of Biological and Environmental Sciences, Kwansei Gakuin University, 1 Gakuen-uegahara, Sanda, Hyogo 669-1330, Japan.

[d] Graduate School of Science, University of Hyogo, 3-2-1 Koto, Kamigori-cho, Ako-gun, Hyogo 678-1297, Japan.

[e] Department of Chemistry, Faculty of Environmental, Life, Natural Science and Technology, Okayama University, Okayama 700-8530, Japan.

[f] Graduate School of Science, The University of Osaka, 1-1 Machikaneyama, Toyonaka, Osaka 560-0043, Japan.

[g] Faculty of Education, Shitennoji University, 3-2-1 Gakuenmae, Habikino, Osaka 583-8501, Japan.

[h] Research Institute for Interdisciplinary Science, Okayama University, Okayama 700-8530, Japan. E-mail: suzuki@okayama-u.ac.jp.

Experimental section

All reagents and solvents were commercially available and used without further purification.

Synthesis of HL^1

To a methanol solution (20 mL) of *p*-hydroxybenzohydrazide (308.5 mg, 2.03 mmol) was added with stirring 3-formyl-6-methyl-chromone (381.5 mg, 2.03 mmol). After the mixture was stirred for 1 h at room temperature, white precipitate formed was collected by filtration and dried in vacuo. Yield: 602.9 mg (91.9%). Anal. Found: C, 66.68; H, 4.66; N, 8.62%. Calcd. for $C_{18}H_{14}N_2O_4$: C, 66.87; H, 4.68; N, 8.66%. ^{1}H NMR (400 MHz, DMSO-d_6, 22 °C): δ 11.74 (s, 1H), 10.15 (s, 1H), 8.79 (s, 1H), 8.60 (s, 1H), 7.93 (dt, *J* = 1.6, 0.8 Hz, 1H), 7.84–7.79 (m, 2H), 7.72–7.62 (m, 2H), 6.88–6.83 (m, 2H), 2.46 (s, 3H).

Synthesis of HL^2

To a methanol solution (20 mL) of *p*-methylbenzohydrazide (221 mg, 1.47 mmol) was added with stirring 3-formyl-6-methyl-chromone (277 mg, 1.47 mmol). The mixture was stirred for 1 h at room temperature, and the resulting white precipitate was collected by filtration and dried in vacuo. Yield: 446 mg (94.5%). Anal. Found: C, 71.20; H, 5.05; N, 8.83%. Calcd. for $C_{19}H_{16}N_2O_3$: C, 71.24; H, 5.03; N, 8.74%. ^{1}H NMR (600 MHz, DMSO-d_6, 22 °C): δ 11.87 (s, 1H), 8.81 (s, 1H), 8.63 (s, 1H), 7.93 (s, 1H), 7.84 (d, J = 7.8 Hz, 2H), 7.69 (dd, J = 8.6, 2.2 Hz, 1H), 7.64 (d, J = 8.6 Hz, 1H), 7.33 (d, J = 7.8 Hz, 2H), 2.45 (s, 3H), 2.38 (s, 3H).

Synthesis of $[Eu(HL^1)_3]Cl_3$ (1Cl)

A solution of HL^1 (54.5 mg, 0.17 mmol) in 2-methoxyethanol (1 mL) was added to a solution of $EuCl_3{\cdot}6H_2O$ (30.6 mg, 0.056 mmol) in 2-methoxyethanol (2 mL), and the mixture was stirred for 1 h at 80 °C. After cooling to ambient temperature, conc. HCl (15 μL) was added, and the reaction mixture was left to stand in a closed vessel with diisopropyl ether. After 1 week colorless needle crystals were obtained. Yield: 64.5 mg (83.9%). Anal. Found: C, 49.95; H, 4.32; N, 5.97%. Calcd. for $C_{57}H_{58}N_6Cl_3EuO_{18}$ (= **1Cl**$\cdot CH_3OC_2H_4OH\cdot 4H_2O$): C, 49.85; H, 4.26; N, 6.12%. FT-IR (KBr / cm^{-1}): ν(N–H) 3236, ν($C{=}N_{imine}$) 1607, ν(C=O) 1577.

Synthesis of [Gd(HL^1)$_3$]Cl_3 (1Gd-Cl)

This gadolinium(III) complex was prepared by a similar method to that for **1Cl** using $GdCl_3 \cdot 6H_2O$, instead of $EuCl_3 \cdot 6H_2O$. Colorless needle crystals. Yield: 79.7 %. Found: C, 50.46; H, 4.23; N, 6.04%. Anal. Calcd. for $C_{60}H_{62.5}N_6Cl_3GdO_{18.25}$ = $[Gd(HL)_3]Cl_3 \cdot 2CH_3OC_2H_4OH \cdot 2.25H_2O$: C, 50.63; H, 4.43; N, 5.90%. FT-IR (KBr / cm^{-1}): ν(N–H) 3236, ν(C=N$_{imine}$) 1607, ν(C=O) 1577.

Synthesis of [Eu(HL^1)$_3$](OTf)$_3$ (1OTf)

A solution of HL^1 (48.3 mg, 0.15 mmol) in chloroform (3 mL) was added to a solution of Eu(OTf)$_3$ (30.0 mg, 0.050 mmol) in acetonitrile (2 mL), and the mixture was stirred for 1 h at room temperature. Diffusion of diisopropyl ether vapor into the reaction mixture gave yellow crystalline products, which were corrected by filtration. Yield: 54.8 mg, 70.2 %. Anal. Found: C, 43.80; H, 3.25; N, 5.01%. Calcd. for $C_{58.5}H_{46}N_6EuF_9O_{21.5}S_3$ (= **1OTf**$\cdot 0.25H_2O \cdot 0.25{}^iPr_2O$): C; 44.02, H; 2.90, N; 5.27. ESI-MS (MeCN): *m/z* 1117.1932. Calcd. for $C_{54}H_{40}N_6EuO_{12}$ [M–2H]$^+$: 1117.1919. FT-IR (KBr / cm^{-1}): ν(N–H) 3239, ν(C=N$_{imine}$) 1604, ν(C=O) 1577, ν(S=O) 1242, ν(C–F) 1030.

Synthesis of [Gd(HL^1)$_3$](OTf)$_3$ (1Gd-OTf)

This gadolinium(III) complex was prepared by a similar method to that for **1OTf** using Gd(OTf)$_3$, instead of Eu(OTf)$_3$. Colorless product. Yield: 71.5 %. Anal. Found: C, 43.79; H, 3.11; N, 5.05%. Calcd. for $C_{58.5}H_{46}N_6GdO_{21.5}S_3$ (= **1Gd-OTf**$\cdot 0.25H_2O \cdot 0.25{}^iPr_2O$): C, 43.88; H, 2.90; N, 5.25%. ESI-MS (MeCN): *m/z* 1122.2010. Calcd. for $C_{54}H_{40}N_6GdO_{12}$ [M–2H]$^+$: 1122.1953. FT-IR (KBr / cm^{-1}): ν(N–H) 3239, ν(C=N$_{imine}$) 1604, ν(C=O) 1573, ν(S=O) 1241, ν(C–F) 1030.

Synthesis of [Eu(HL^2)$_3$](OTf)$_3$ (2OTf)

A solution of HL^2 (48.3 mg, 0.15 mmol) in acetone (1 mL) was added to a solution of Eu(OTf)$_3$ (30.0 mg, 0.050 mmol) in acetone (2 mL), and the mixture was stirred for 1 h at room temperature. Diffusion of diethyl ether vapor into the resulting solution gave yellow crystalline product, which was collected by filtration. Colorless needle crystals were obtained by slow diffusion of layered hexane into a dichloromethane solution. Yield: 54.8 mg, 70.2 %. Anal. Found: C, 46.09; H, 3.12; N, 5.26%. Calcd. for $C_{60}H_{48}N_6EuF_9O_{18}S_3$ (= **2OTf**): C, 46.19; H, 3.10; N, 5.39%. ESI-MS (MeCN): *m*/*z* 1111.2547. Calcd. for $C_{57}H_{46}N_6EuO_9$ $[M–2H]^+$: 1111.2541. FT-IR (KBr / cm^{-1}): ν(N–H) 3239, ν($C=N_{imine}$) 1609, ν(C=O) 1573, ν(S=O) 1241, ν(C–F) 1029.

Synthesis of $[Gd(HL^2)_3](OTf)_3$ (2Gd-OTf)

This complex was prepared by a similar method to that for **2OTf** using $Gd(OTf)_3$, instead of $Eu(OTf)_3$. Yield: 75.1 %. Anal. Found: C, 46.38; H, 3.30; N, 5.26%. Calcd. for $C_{60}H_{48}N_6EuF_9O_{18}S_3$ (= **2Gd-OTf**): C, 46.03; H, 3.09; N, 5.37%. ESI-MS (MeCN): *m*/*z* 1116.2602. Calcd. for $C_{57}H_{46}N_6GdO_9$ $[M–H]^+$: 1116.2576. FT-IR (KBr / cm^{-1}): ν(N–H) 3239, ν($C=N_{imine}$) 1608, ν(C=O) 1573, ν(S=O) 1241, ν(C–F) 1029.

Synthesis of $[Y(HL^2)_3](OTf)_3$ (2Y-OTf)

This complex was prepared by a similar method to that for **2OTf** using $Y(OTf)_3$, instead of $Eu(OTf)_3$. Yield: 72.4%. Anal. Found: C, 46.70; H, 3.32; N, 5.40. Calcd. for $C_{60.75}H_{49.5}N_6Cl_{1.5}F_9YO_{18}S_3$ (= **2Y-OTf**·$0.75CH_2Cl_2$): C, 46.75; H, 3.20; N, 5.38%. ESI-MS (MeCN): *m*/*z* 1047.2402. Calcd. for $C_{57}H_{46}N_6YO_9$ $[M–2H]^+$: 1047.2379. FT-IR (KBr / cm^{-1}): ν(N–H) 3239, ν($C=N_{imine}$) 1608, ν(C=O) 1574, ν(S=O) 1242, ν(C–F) 1029.

Measurements.

The ^1H NMR spectra were acquired using Varian NMR System 600 and 400-MR spectrometers at 22 °C. The chemical shifts were referenced to the residual solvent peaks. ESI-MS spectra were obtained from Bruker ESI-Qq-TOF-MS compact spectrometer. Elemental analyses were performed at the Advanced Science Research Center, Okayama University. Infrared spectra were recorded on a Jasco FT/IR-4X spectrophotometer with the samples prepared as KBr disks. UV-vis absorption spectra were recorded on a Jasco V-550 or V-750 spectrophotometer. Luminescence and excitation spectra were measured using a Jasco FP-6300 or FP-8600. The absolute luminescence quantum yields were determined on a Hamamatsu Photonics C9920-02 absolute photoluminescence quantum yield measurement system spectrometer or FP-8500 using Jasco ILFC-847 as an integrating sphere. Luminescence lifetimes were recorded by Hamamatsu Quantaurus-tau C11367 compact fluorescence spectrometer. All solutions for photophysical data measurements were degassed under N_2 prior to use unless otherwise noted.

Crystallography

Each single-crystal of complexes **1Cl**, **1OTf**, **2OTf, 1Gd-Cl, 2Gd-OTf** or **2Y-OTf** was mounted with a cryoloop and flash cooled using a cold nitrogen stream. The X-ray diffraction data were obtained at 188(2) or 100(2) K using a Rigaku R-axis rapid imaging plate detector with a graphite-monochromated Mo Kα radiation ($\lambda = 0.71073$ Å), a Rigaku Vari-Max diffractometer with a Hypix CCD detector and a Mo Kα radiation ($\lambda = 0.71073$ Å) monochromated by multi-mirror, or synchrotron radiation ($\lambda = 0.4108$ Å) at BL02B1 of Spring-8. An empirical absorption correction was applied. The structures were solved by a direct method with SHELXT program using the Olex2 1.5 software package.[1] All non-hydrogen atoms were refined anisotropically using full-matrix least-squares method based on F^2 with SHELXL program.[2] Hydrogen atoms (except for those of solvent H_2O and alcoholic O–H, which were not included in the calculation) were located at theoretical positions and refined as riding atoms. Isotropic displacement parameters were set to $U_{\mathrm{iso}} = 1.2\ U_{\mathrm{eq}}$ of the parent atoms. For the analysis of **1OTf**·$^{i}Pr_2O$, owing to large voids (ca. 3045 Å^3 per unit cell), solvent molecules assuming free water molecules were treated using the MASK procedure implemented in Olex2 (equivalent to PLATON/SQUEEZE), removing approximately 447 electrons per unit cell. This corresponds to ca. 3 water molecules per formula unit ($Z = 8$).

The powder X-ray diffraction (PXRD) data were collected on a Rigaku RINT-TTR III diffractometer at room temperature. The crystalline samples were dried in air and ground in an agate mortar before mounting for the measurement.

Calculation of the luminescence quantum yield[3,4]

The transitions of $^5D_0 \rightarrow {}^7F_{0,2,3,4}$ are electronic dipole transitions, and their intensities vary with the symmetry of coordination environment around the Eu^{III} center. On the other hand, the $^5D_0 \rightarrow {}^7F_1$ transition is a magnetic dipole transition and is not affected by the coordination environment. Thus, it is assumed that the dipole strength and the energy of the $^5D_0 \rightarrow {}^7F_1$ transition are constant.

The radiative rate constant is formulated as:

$$k_r^{Eu} = A_{\mathrm{MD},0} \cdot n^3 (I_{\mathrm{tot}}/I_{\mathrm{MD}}),$$

where $A_{\mathrm{MD},0}$, n, and $(I_{\mathrm{tot}}/I_{\mathrm{MD}})$ are representing the spontaneous luminescence rate of the $^5D_0 \rightarrow {}^7F_1$ transition in vacuo, refractive index of the medium, and ratio of the total $^5D_0 \rightarrow {}^7F_J$ area of the Eu$^{\mathrm{III}}$ luminescence spectrum to the area of the $^5D_0 \rightarrow {}^7F_1$ transition band, respectively.

The observed decay rate constant (k_{obs}) of the $^5D_0$ state is given as:

$$k_{Obs} = 1/\tau_{Obs} = k_r^{Eu} + k_{nr}^{Eu},$$

where τ_{Obs}, k_r^{Eu} and k_{nr}^{Eu} are the observed lifetime of the $^5D_0$ state, the radiative rate constant of Eu$^{\mathrm{III}}$, and non- radiative rate constant of Eu$^{\mathrm{III}}$, respectively.

The quantum yield of Eu$^{\mathrm{III}}$ luminescence (Φ_{Eu}) and overall photosensitization efficiency (Φ_{tot}) were determined as follows:

$$\Phi_{Eu} = k_r^{Eu} / (k_r^{Eu} + k_{nr}^{Eu}) = k_r^{Eu} / k_{obs}$$

$$\Phi_{tot} = \eta_{sens} \times \Phi_{Eu} .$$

Table S1 Crystallographic data.

Compounds	**1Cl**·1.5H_2O ·$CH_3OC_2H_4OH$	**1OTf**·${}^{i}Pr_2O$ (solvent masked)	**2OTf**·H_2O·3CH_2Cl_2	**1Gd-Cl**·0.5H_2O ·$CH_3OC_2H_4OH$	**2Gd-OTf**·H_2O ·2.75CH_2Cl_2
CCDC deposition no.	2532337	2532338	2532339	2532340	2532341
Chemical Formula	$C_{57}H_{53}Cl_3EuN_6O_{15.5}$	$C_{63}H_{56}EuF_9N_6O_{22}S_3$	$C_{63}H_{56}Cl_6EuF_9N_6O_{19}S_3$	$C_{57}H_{51}Cl_3GdN_6O_{14.5}$	$C_{62.75}H_{55.5}Cl_{5.5}GdF_9N_6O_{19}S_3$
Formula Weight	1328.39	1668.27	1832.99	1315.66	1817.05
T / K	188(2)	100(2)	100(2)	188(2)	100(2)
Crystal Color and Shape	colorless, needle	colorless, plate	colorless, needle	colorless, needle	colorless, needle
Crystal System	monoclinic	monoclinic	triclinic	monoclinic	triclinic
Space Group , Z	*Cc*, 4	*C*2/*c*, 8	$P\bar{1}$, 2	*Cc*, 4	$P\bar{1}$, 2
Size of Specimen / mm	0.46 × 0.10 × 0.10	0.27 × 0.20 × 0.07	0.56 × 0.11 × 0.09	0.50 × 0.07 × 0.07	0.50 × 0.09 × 0.06
a / Å	12.5079(7)	36.4018(4)	11.9562(4)	12.41539(17)	12.0010(4)
b / Å	29.639(2)	13.99670(10)	13.7396(3)	29.415(4)	13.6463(3)
c / Å	17.5195(11)	34.1043(3)	25.1436(6)	17.640(3)	25.1879(6)
α / °	90	90	83.022(2)	90	83.336(2)
β / °	106.5524(18)	116.3560(10)	83.755(2)	106.467(4)	82.998(2)
γ / °	90	90	77.632(2)	90	77.727(2)
V / Å^3	6225.7(7)	15570.1(3)	3990.07(19)	6177.9(14)	3983.36(19)
D_{calc} / g cm^{-3}	1.388	1.423	1.524	1.415	1.513
μ(Mo Kα) / mm^{-1}	1.198	0.242	1.154	1.270	1.184
$R_1[I > 2\sigma(I)]$	0.0688	0.0569	0.0561	0.0799	0.0563
wR_2 [all data]	0.2059	0.1770	0.1535	0.2270	0.1673
Flack Parameter	–0.001(8)	–	–	0.021(14)	–

Table S2 Photophysical properties of the (fully protonated and mono-deprotonated) Eu^{III} complexes in the solid state and in acetonitrile.

Complex	Sample states	Φ_{tot}	Φ_{Eu}	τ_{obs}/ms	k_{r}^{Eu}/s^{-1}	k_{nr}^{Eu}/s^{-1}	η_{sens}
1Cl	Solid	0.56	0.56	0.76	76.9	546	>0.99
1Cl after heating ($[Eu(L^1)(HL^1)_2]Cl_2$)	Solid	0.00†	—	—	—	—	—
1OTf	Solid	0.57	0.57	0.53	71.3	140	>0.99
1OTf	CH_3CN	0.03	0.32	0.70	45.0	974	0.09
1OTf with Et_3N ($[Eu(L^1)(HL^1)_2]^{2+}$)	CH_3CN	0.00†	—	—	—	—	—
2OTf	Solid	0.40	0.57	0.74	77.2	587	0.70
2OTf	CH_3CN	0.01>	0.34	0.74	46.5	888	0.02
2OTf with Et_3N ($[Eu(L^2)(HL^2)_2]^{2+}$)	CH_3CN	0.00†	—	—	—	—	—

† Below the detection limit.

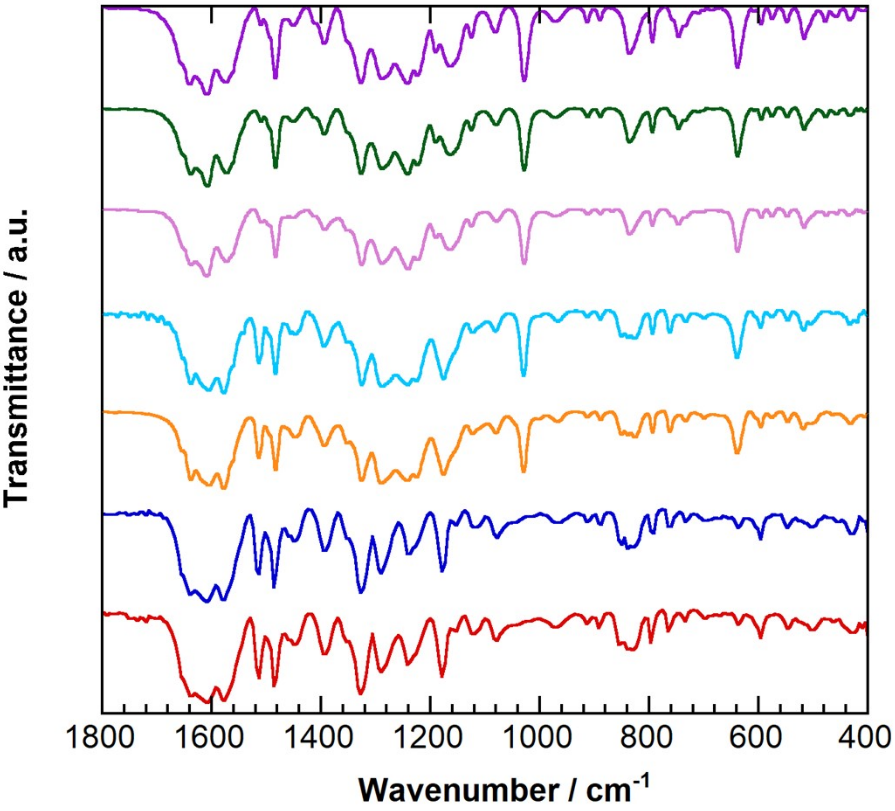

Fig. S1 FT-IR spectra of **1Cl** (red), **1Gd-Cl** (blue), **1OTf** (orange), **1Gd-OTf** (sky blue), **2OTf** **(**pink), **2Gd-OTf** (green) and **2Y-OTf** (purple).

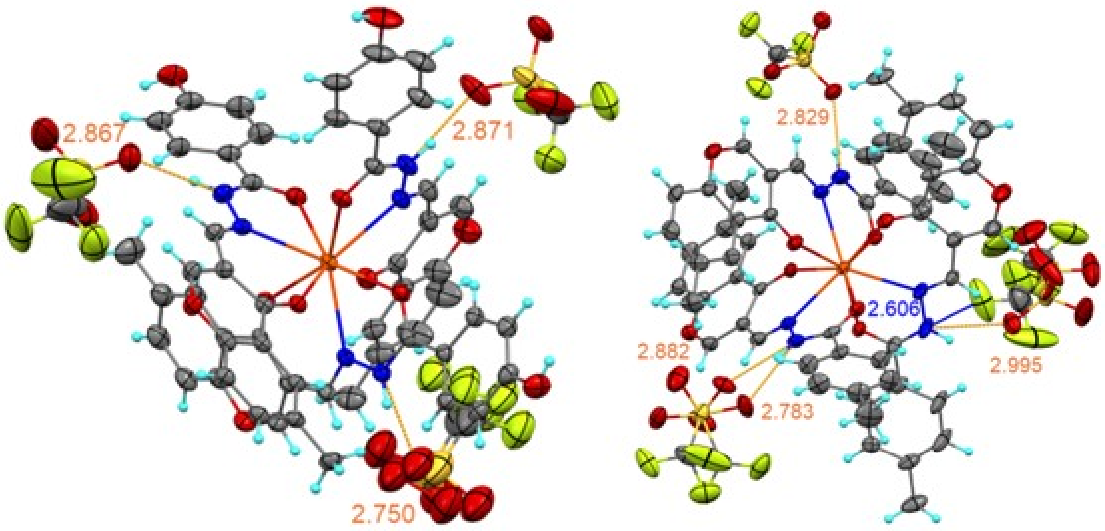

Fig. S2 ORTEP drawings (the thermal ellipsoids at 50 % probability level) of the cationic complexes and the surrounding OTf⁻ anions bonded to the hydrazone N–H protons by hydrogen bonds in **1OTf** (left) and **2OTf** (right).

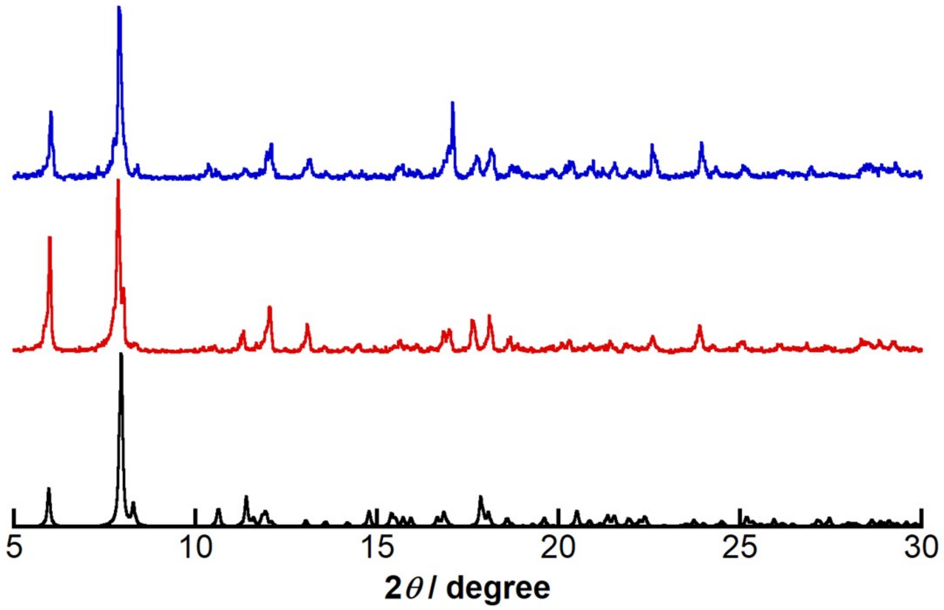

Fig. S3 Powder X-ray diffraction spectra of simulated **1Cl** (black), observed **1Cl** (red) and **1Gd-Cl** (blue).

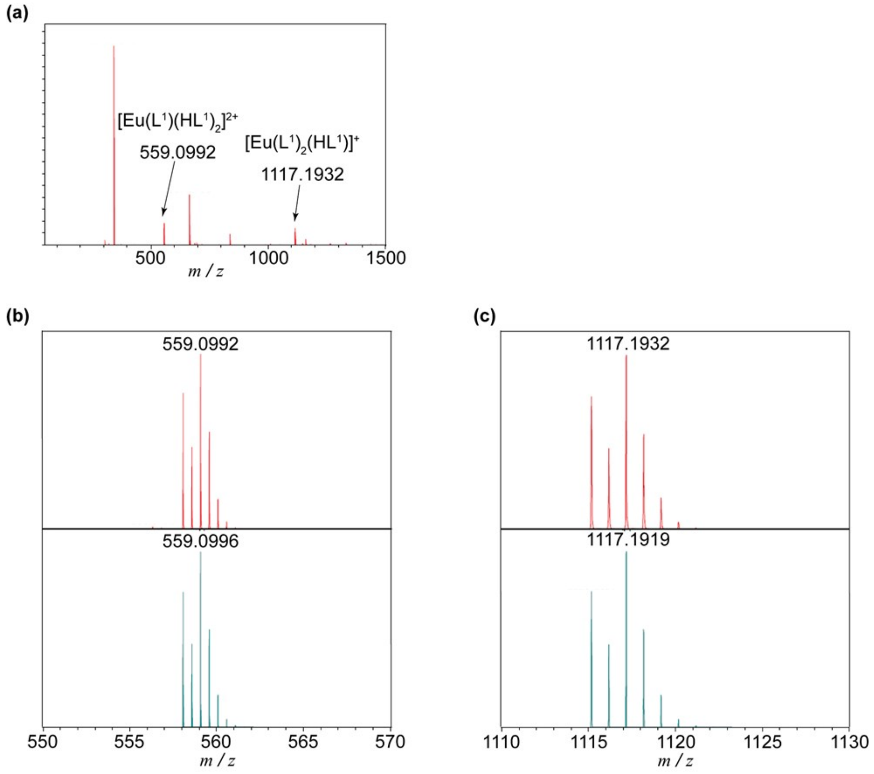

Fig. S4 (a) ESI-MS spectrum of **1OTf** in acetonitrile. Comparison of experimental (red) and simulated (green) molecular ion envelopes of (b) $[Eu(L^1)(HL^1)_2]^{2+}$ and (c) $[Eu(L^1)_2(HL^1)]^{+}$.

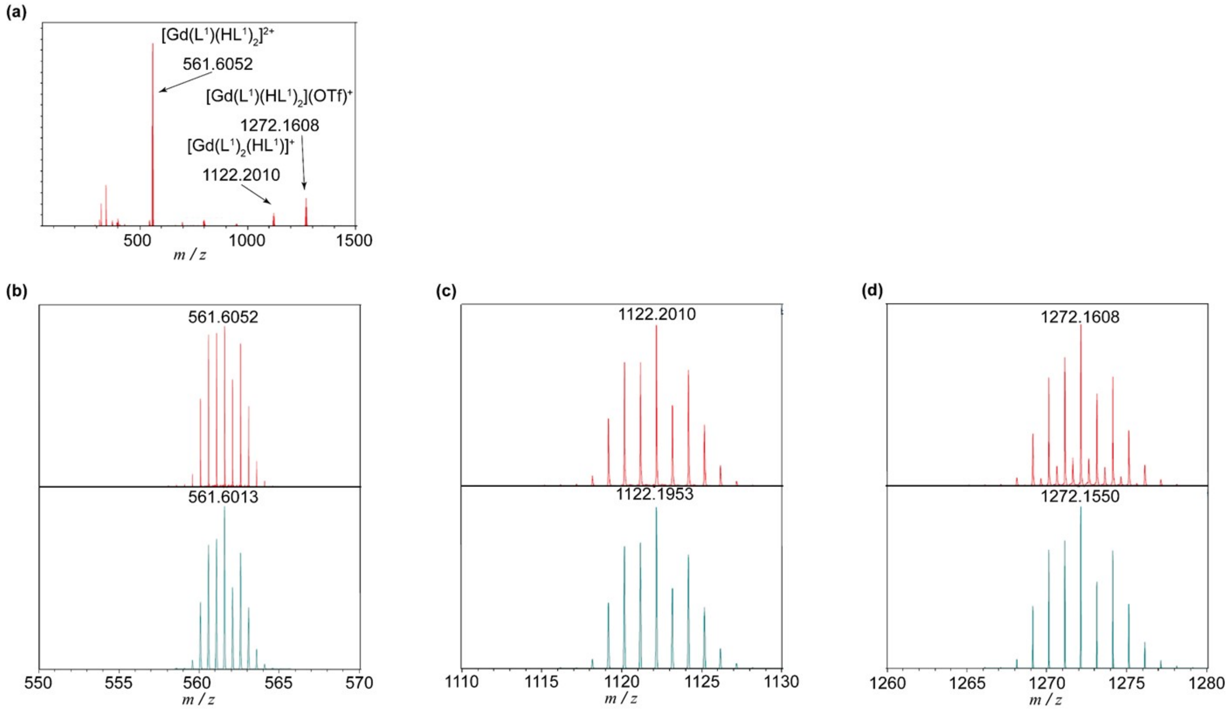

Fig. S5 (a) ESI-MS spectrum of **1Gd-OTf** in acetonitrile. Comparison of experimental (red) and simulated (green) molecular ion envelopes of (b) $[Gd(L^1)(HL^1)_2]^{2+}$, (c) $[Gd(L^1)_2(HL^1)]^+$ and (d) $[Gd(L^1)(HL^1)_2](OTf)^+$.

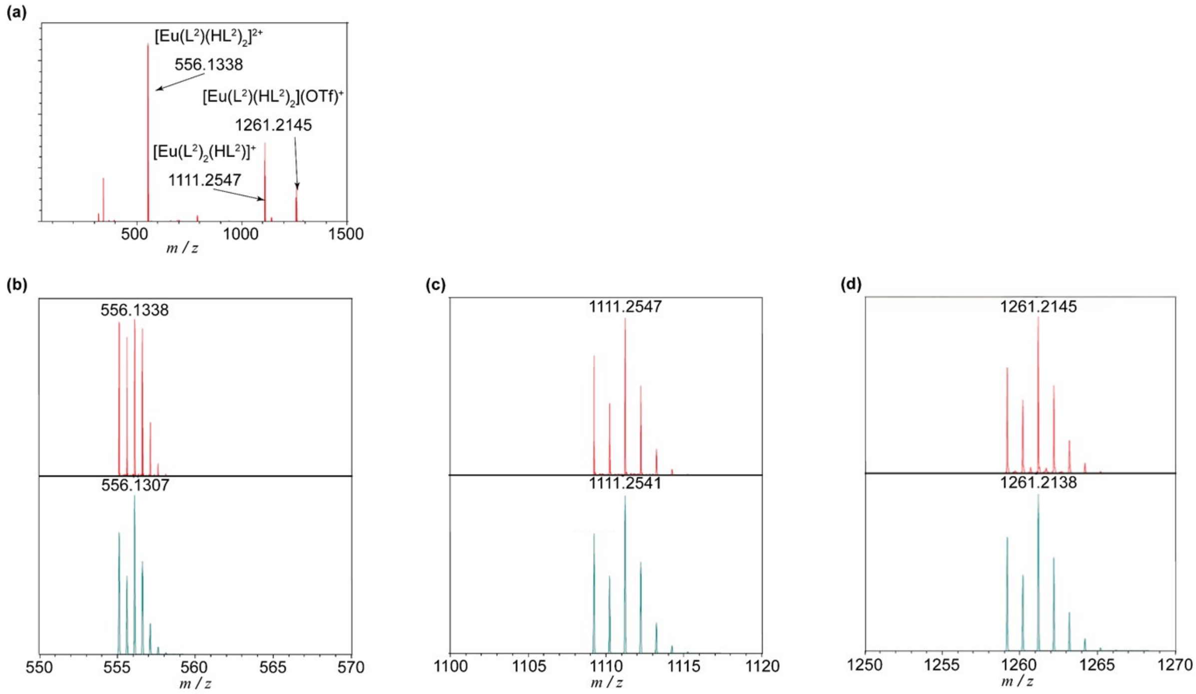

Fig. S6 (a) ESI-MS spectrum of **2OTf** in acetonitrile. Comparison of experimental (red) and simulated (green) molecular ion envelopes of (b) $[Eu(L^2)(HL^2)_2]^{2+}$, (c) $[Eu(L^2)_2(HL^2)]^+$ and (d) $[Eu(L^2)(HL^2)_2](OTf)^+$.

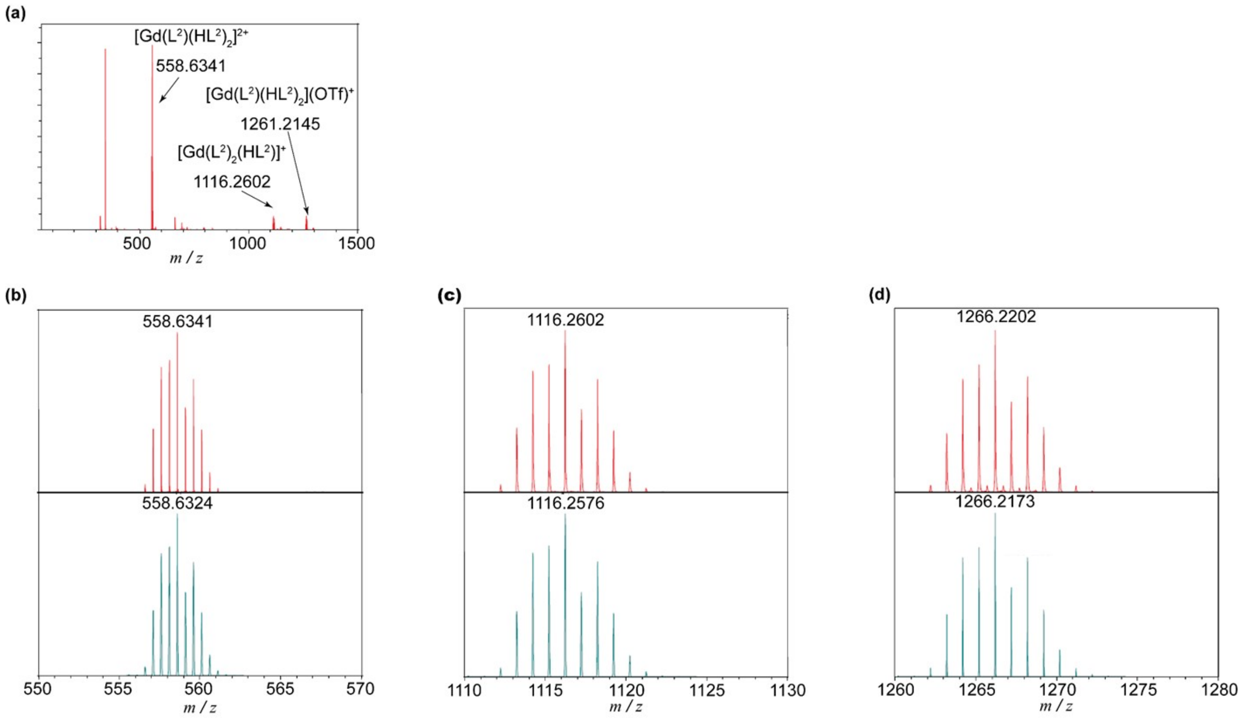

Fig. S7 (a) ESI-MS spectrum of **2Gd-OTf** in acetonitrile. Comparison of experimental (red) and simulated (green) molecular ion envelopes of (b) $[Gd(L^2)(HL^2)_2]^{2+}$, (c) $[Gd(L^2)_2(HL^2)]^+$ and (d) $[Gd(L^2)(HL^2)_2](OTf)^+$.

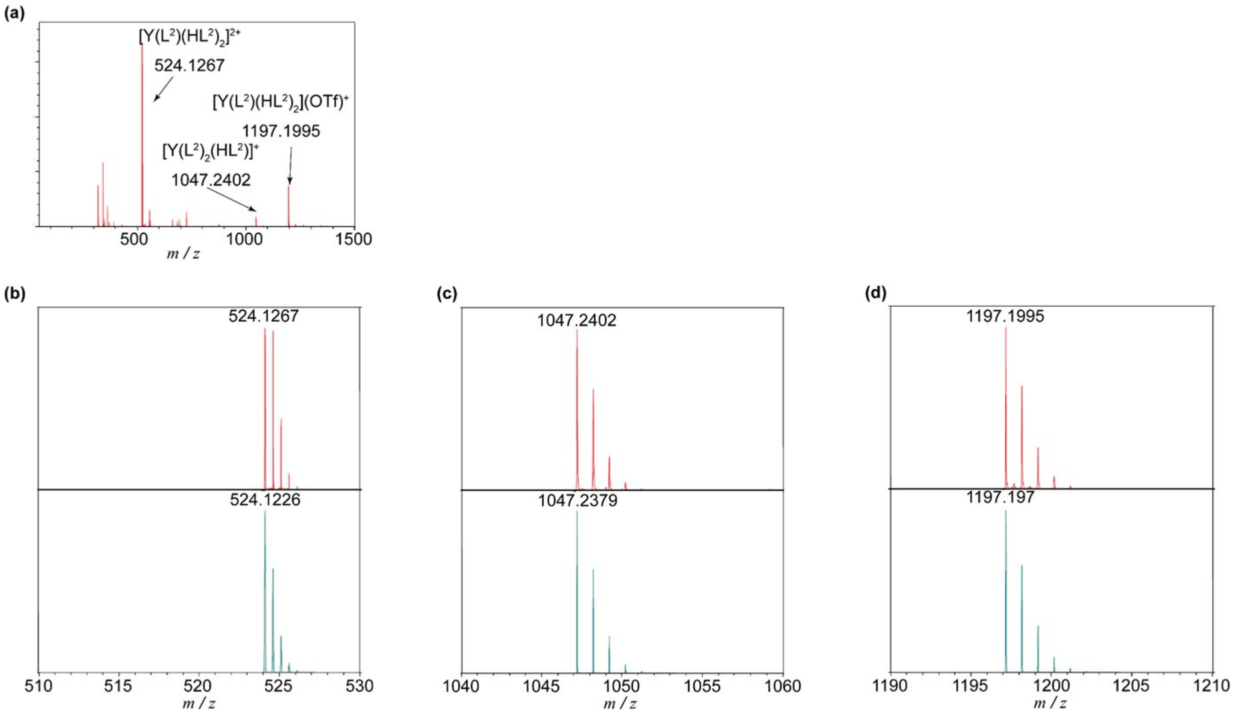

Fig. S8 (a) ESI-MS spectrum of **2Y-OTf** in acetonitrile. Comparison of experimental (red) and simulated (green) of molecular ion envelopes of (b) $[Y(L^2)(HL^2)_2]^{2+}$, (c) $[Y(L^2)_2(HL^2)]^+$ and (d) $[Y(L^2)(HL^2)_2](OTf)^+$.

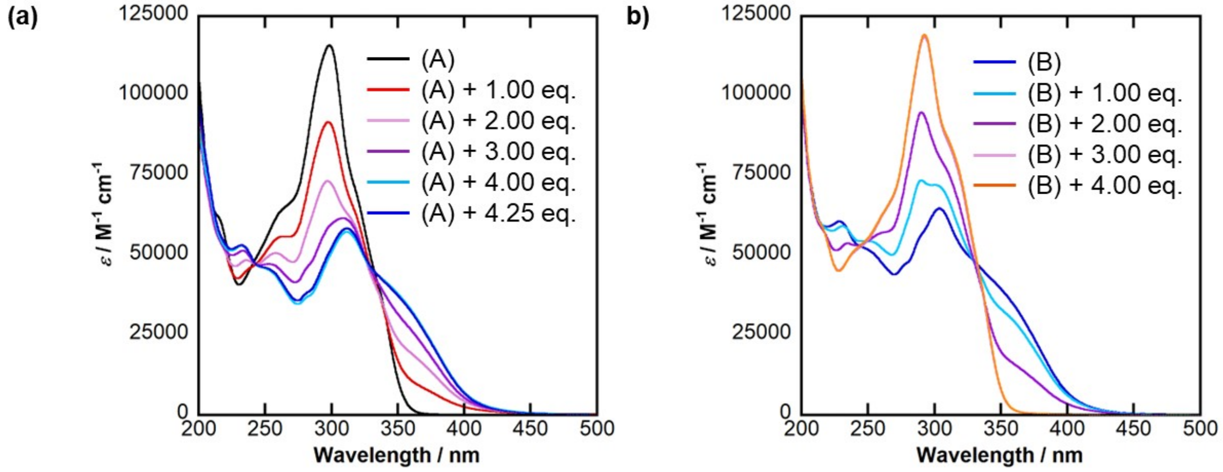

Fig. S9 Absorption spectral change of (a) **2OTf** and 1.0 eq. $HClO_4$ in acetonitrile {solution(A)} by addition of TEA and that of (b) **2OTf**, 1.0 eq. $HClO_4$ and 4.0 eq. TEA in acetonitrile (blue) {solution(B)} by addition of $HClO_4$.

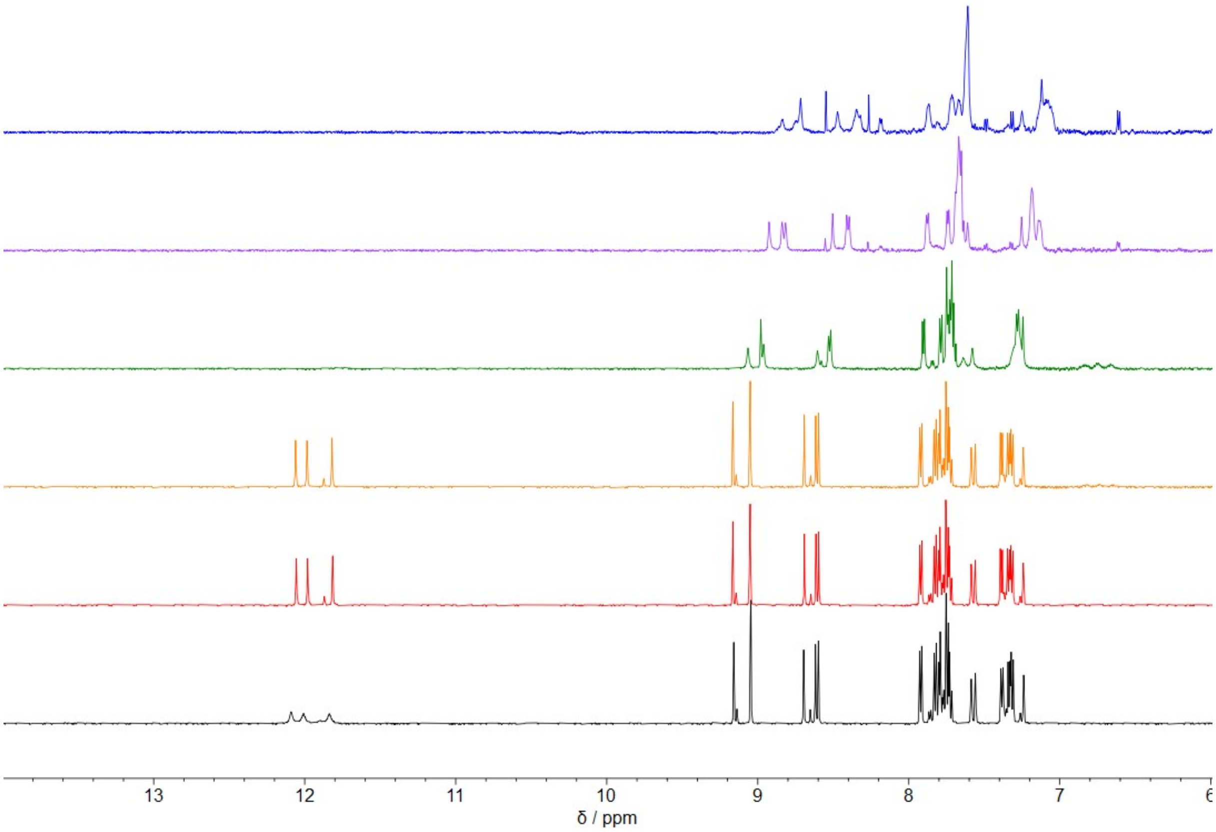

Fig. S10 ^{1}H NMR spectral of (black) **2Y-OTf** in acetonitrile-d_3, and those with (red) 1.0 eq. $HClO_4$; (orange) 1.0 eq. $HClO_4$ and 1.0 eq. TEA; (green) 1.0 eq. $HClO_4$ and 2.0 eq. TEA; (purple) 1.0 eq. $HClO_4$ and 3.0 eq. TEA; and (blue) 1.0 eq. $HClO_4$ and 4.0 eq. TEA.

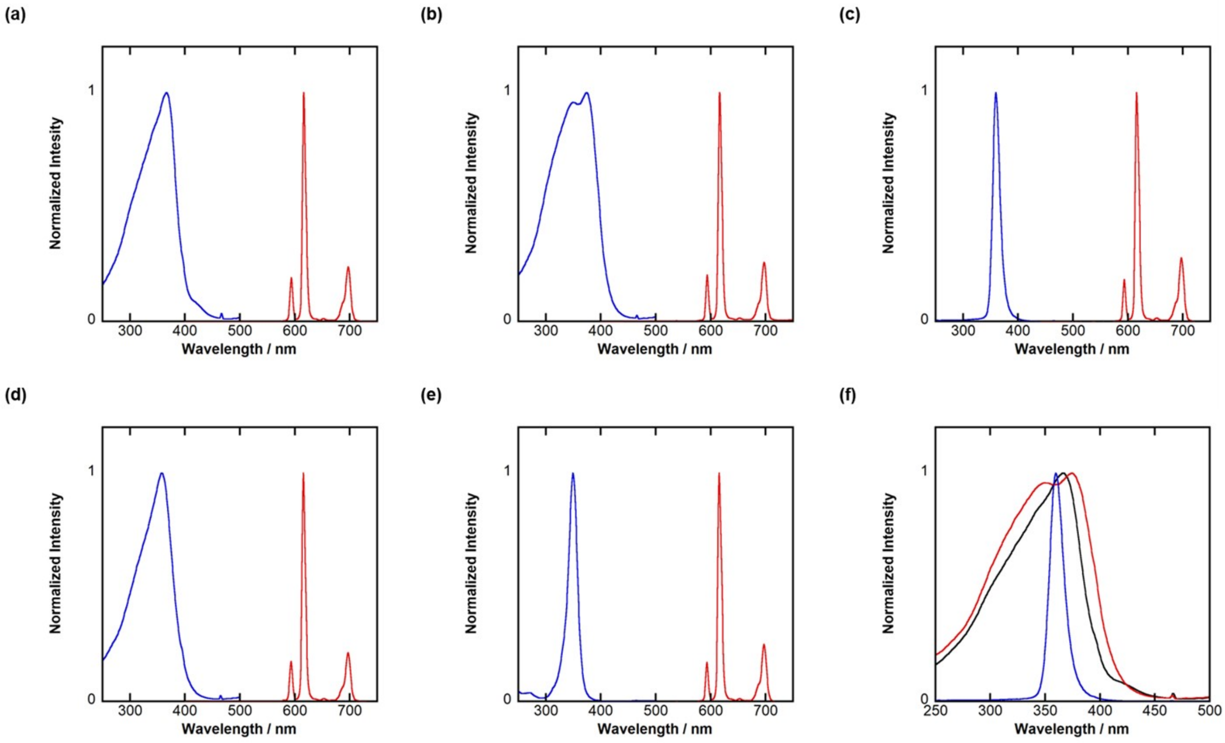

Fig. S11 Photoluminescence (red, λ_{ex} = 350 nm) and excitation (blue, λ_{em} = 616 nm) spectra of the Eu^{III} complexes: (a) **1Cl** in the solid state, (b) **1OTf** in the solid state, (c) **1OTf** in acetonitrile, (d) **2OTf** in the solid state and (e) **2OTf** in acetonitrile. (f) A comparison of excitation spectra of **1Cl** (black) and **1OTf** (red) in the solid state and **1OTf** in acetonitrile (blue) **(**λ_{em} = 616 nm**)**.

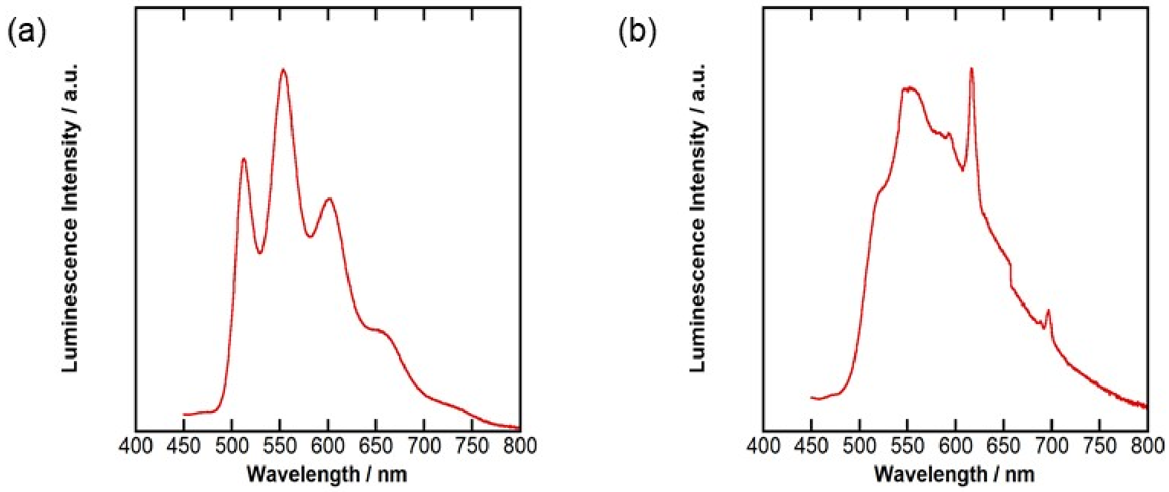

Fig. S12 Photoluminescence spectra of (a) **1Gd-Cl** and **(b) 2Gd-OTf** in the solid states (λ_{ex} = 390 nm).

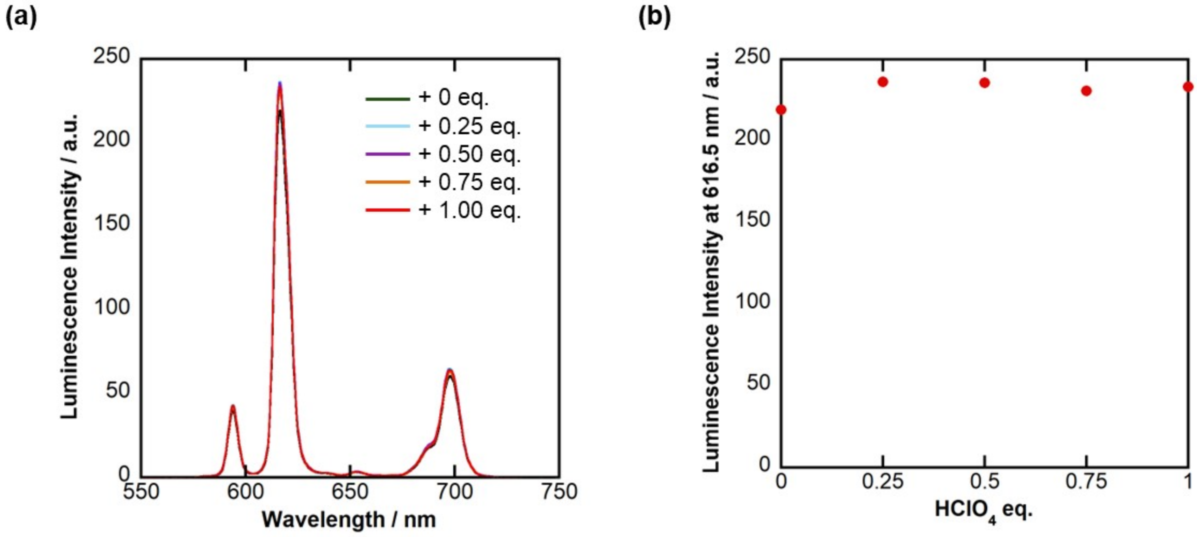

Fig. S13 (a) Photoluminescence (λ_{ex} = 360 nm) spectral change of **1OTf** (9.7×10^{-5}M) in acetonitrile by titration of $HClO_4$. (b) The intensity of the luminescence at 616.5 nm by titration of $HClO_4$ (0–1.0 eq.).

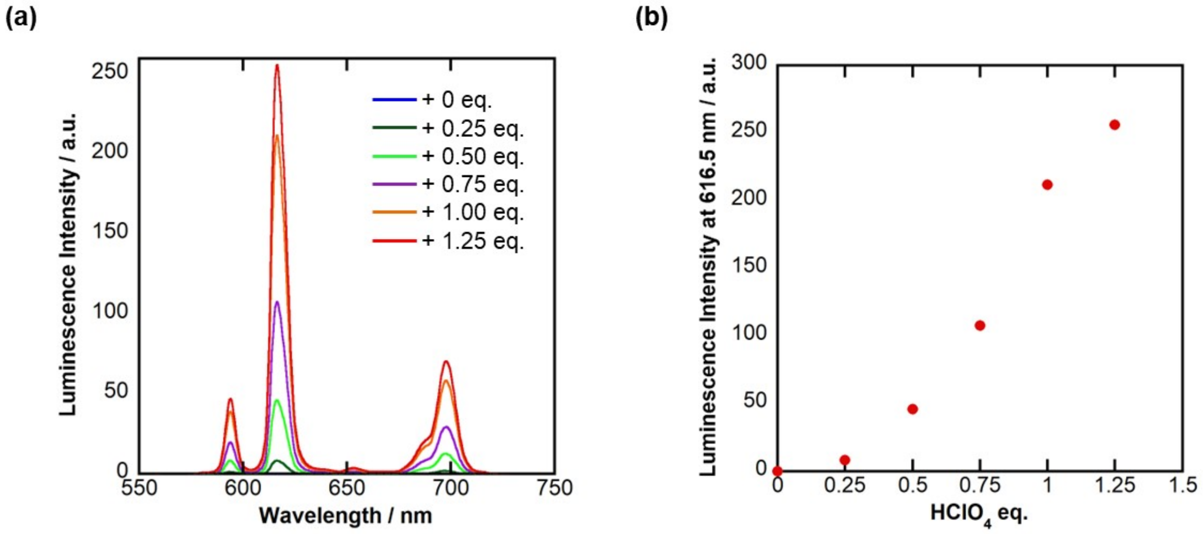

Fig. S14 (a) Photoluminescence (λ_{ex} = 360 nm) spectral change of **1OTf** (9.7×10^{-5}M) with 1.0 eq. $HClO_4$ and 2.25 eq. TEA in acetonitrile by titration of $HClO_4$. (b) The intensity of the luminescence at 616.5 nm by titration of $HClO_4$ (0–1.25 eq.).

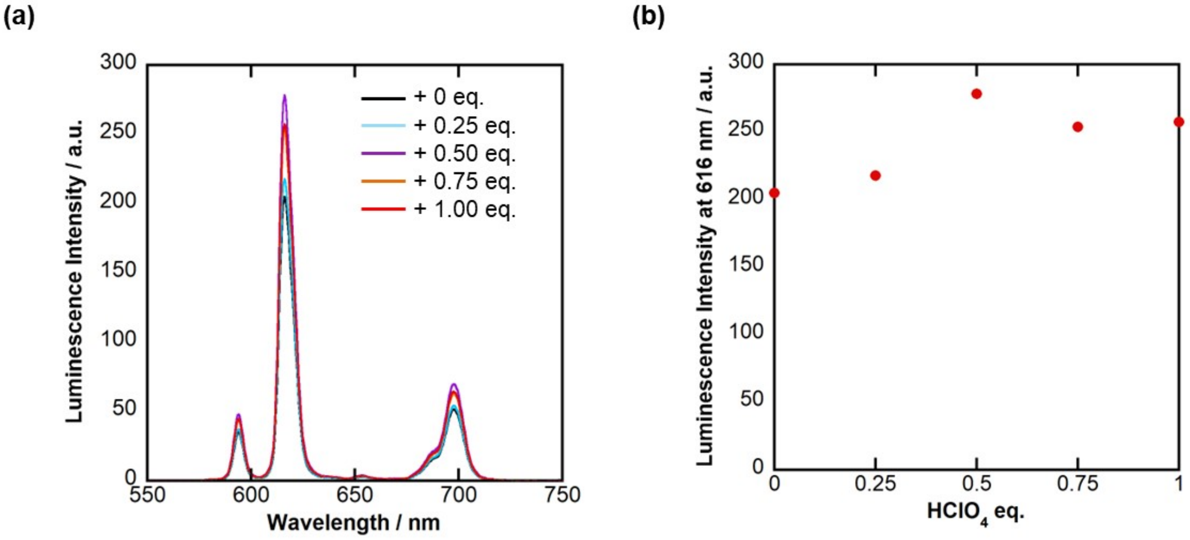

Fig. S15 (a) Photoluminescence (λ_{ex} = 360 nm) spectral change of **2OTf** (1.0×10^{-4}M) in acetonitrile by titration of $HClO_4$. (b) The intensity of the luminescence at 616 nm by titration of $HClO_4$ (0–1.0 eq.).

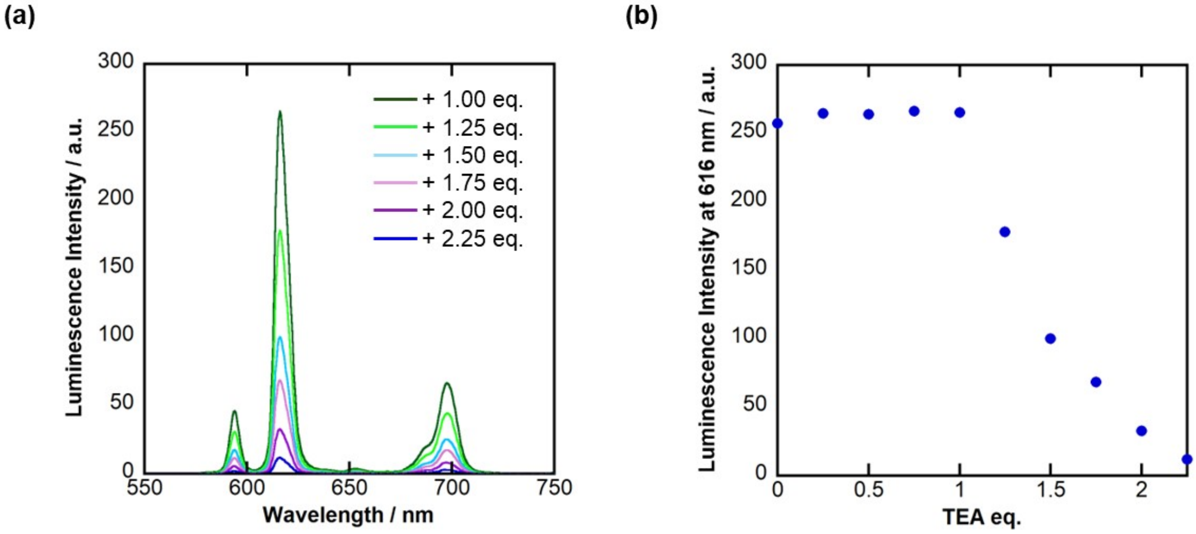

Fig. S16 (a) Photoluminescence (λ_{ex} = 360 nm) spectral change of **2OTf** (1.0×10^{-4}M) with 1.0 eq. $HClO_4$ in acetonitrile by titration of TEA. (blue). (b) The intensity of the luminescence at 616.5 nm by titration of TEA (0–2.25 eq.).

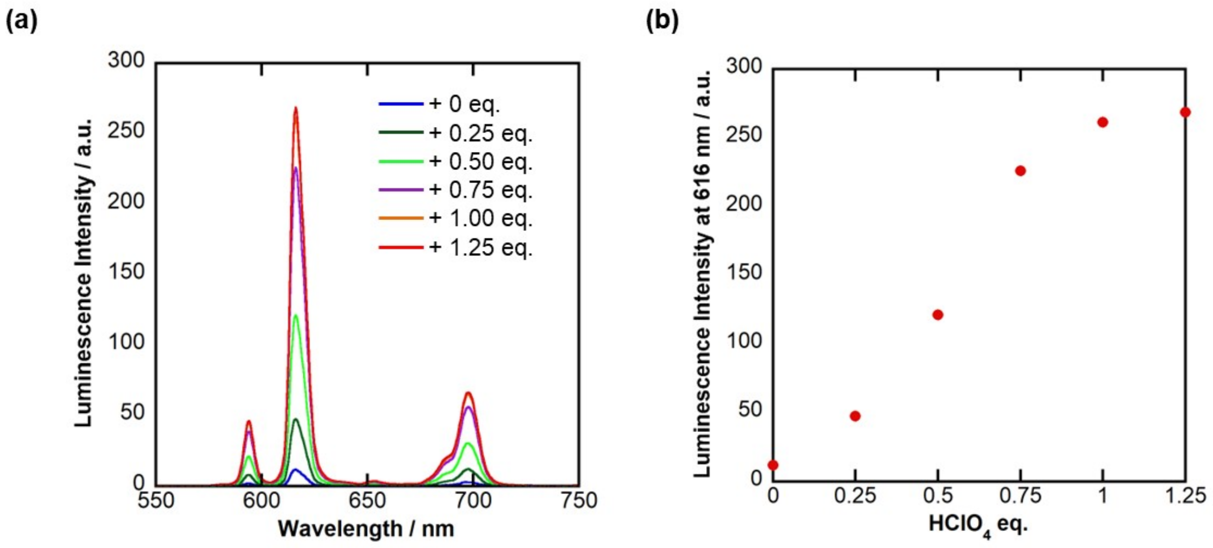

Fig. S17 (a) Photoluminescence (λ_{ex} = 360 nm) spectral change of **2OTf** (1.0×10^{-4}M) with 1.0 eq. $HClO_4$ and 2.25 eq. TEA in acetonitrile by titration of $HClO_4$. (b) The intensity of the luminescence at 616.5 nm by titration of $HClO_4$ (0–1.25 eq.).

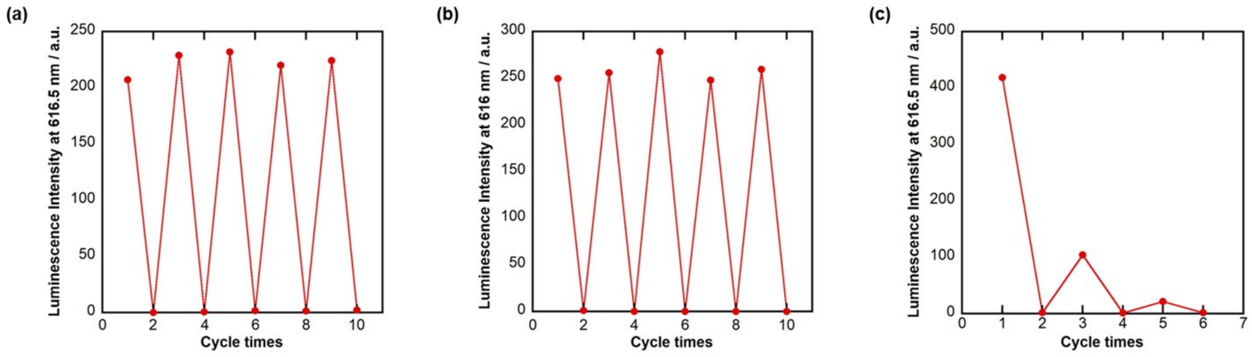

Fig. S18 Repeated switching (on/off) tests of luminescence intensity at 616.5 nm for (a) **1OTf** and (b) **2OTf** in acetonitrile by addition of base (NEt_3) and acid (HCl), and that for (c) **1Cl** in the solid state by heating and exposure of HCl vapor.

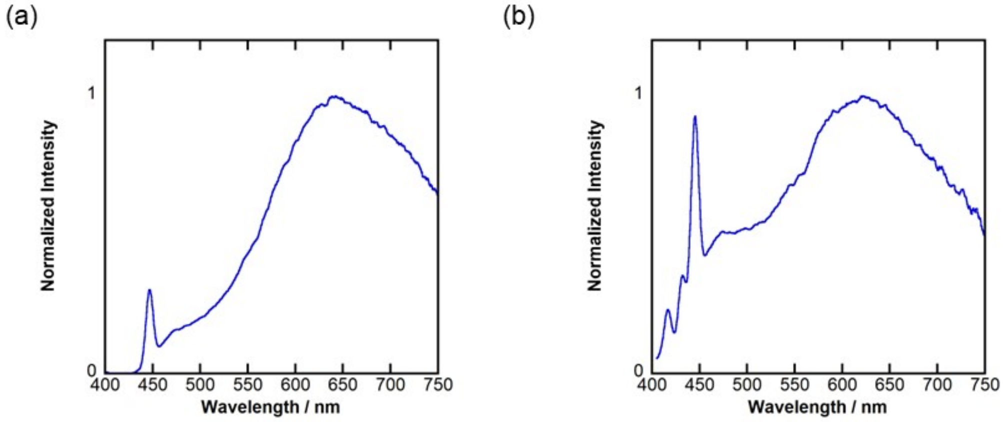

Fig. S19 Phosphorescence spectra (λ_{ex} = 400 nm) of (a) **1Gd-OTf** and (b) **2Gd-OTf** in acetonitrile with 1.0 eq. $HClO_4$ and 2.25 eq. TEA. Note that the spectrum at 450 nm is due to the Raman signal of solvent acetonitrile.

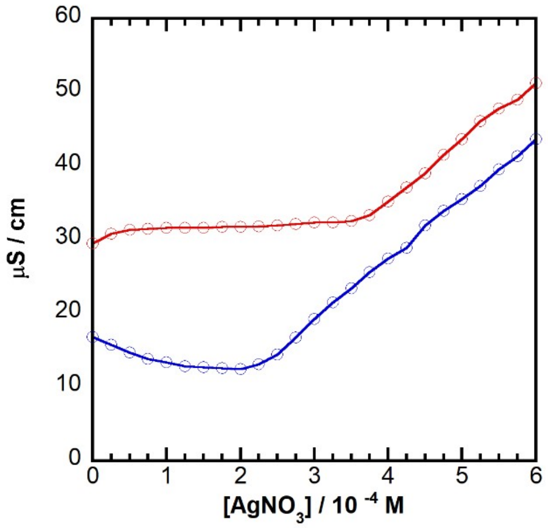

Fig. S20 Change in the electrical conductivity of a methanol solution of **1Cl** (1.0×10^{-4} M) by addition of an methanolic solution of $AgNO_3$ (1.0×10^{-4} M): red, **1Cl**; blue, after heating sample at 140 °C for 5 min).

Reference

1 Dolomanov, O. V.; Bourhis, L. J.; Gildea, R. J.; Howard, J. A. K. and Puschmann, H. OLEX2: A Complete Structure Solution, Refinement and Analysis Program. *J. Appl. Crystallogr.*, 2009, **42**, 339–341.

2 Sheldrick, G. A Short History of SHELX. *Acta Crystallogr.*, *Sect. A: Found. Crystallogr.*, 2008, **64**, 112–122.

3 Werts, M. H. V.; Jukes, R. T. F. and Verhoeven, J. W. *Phys. Chem. Chem. Phys.*, 2002, **4**, 1542–1548.

4 Miyazaki, S.; Gotanda, M.; Kitagawa, Y.; Hasegawa, Y.; Miyata, K. and Onda, K. *J. Phys. Chem. Lett.*, 2024, **15**, 10718–10724.